7(b). Microbial mat features in terrigenous clastics of the Belt Supergroup, Mid-Proterozoic of Montana, USA

Juergen Schieber

Deposited between 1450 and 850 Ma (Harrison, 1972), the Belt Supergroup of Montana (Fig. 7(b)-1) forms a thick and primarily terrigenous clastic succession (Fig. 7(b)-2). Although today located on continental crust, initially the Belt basin probably formed a narrow gulf that was connected to the Proterozoic ocean (Cressman, 1989). The oldest sedimentary unit, the Prichard Formation (Fig. 7(b)-2), has been interpreted as a turbidite succession and was probably deposited in comparatively deep water (Cressman, 1989). The basin shallowed towards the end of Prichard deposition, and then was filled with shallow water to subaerial deposits for the remainder of Belt sedimentation (Winston, 1986). A lacustrine depositional model has been proposed by Winston (1986) on the basis of facies comparisons with the lacustrine Green River Formation (Eocene) of Wyoming. However, the lacustrine hypothesis conflicts with Cressman's (1989) work that suggests a gulf connected to the Proterozoic ocean. Geochemical considerations, such as chemical mass balances for the various formations and the problem of sourcing the large quantities of calcium and magnesium in the Middle Belt Carbonate, indicate that even though deposition was epicratonic, the basin was nonetheless in communication with the Proterozoic ocean (Schieber, 1998a). In this chapter we will survey microbial mat-related features observed in shales and sandstones of most of the Belt succession. Illustrated examples are from the Newland Formation, the Revett Formation, the Mt. Shields Formation, and the McNamara Formation (Fig. 7(b)-2). They have been described in significantly more detail in prior publications (Schieber, 1986, 1998b, 1999).

Newland Formation: striped shales

Offshore shales in the Newland Formation of the eastern Belt basin (Schieber, 1985) have a characteristic striped appearance that has been interpreted as indicative of microbial mat colonization of a muddy substrate (Schieber, 1986). In outcrop, dark gray to reddish-brown shale beds, a few millimetres to some centimetres in thickness, alternate with beds of gray shale (Fig. 7(b)-3, Fig. 7(b)-4A) that measure some millimetres to centimetres in thickness and may have silt or shale intraclasts at the base. Comparison of outcrop and and drill core specimens (Fig. 7(b)-4B, -4C) shows that the dark gray to reddish-brown beds are the weathered equivalent of carbonaceous silty shale beds with abundant (several percent) scattered pyrite grains, and that the gray beds are clay-dominated with minor amounts of pyrite and organic matter (Schieber, 1989).

Although the wavy-crinkly internal laminae (Fig. 7(b)-4D) of the carbonaceous beds hint at a possible microbial mat origin, the most convincing evidence for the microbial mat character of these beds is their behaviour during soft sediment deformation and erosion. During soft sediment deformation and erosion, carbonaceous beds and laminae behaved like tough leathery membranes (Fig. 7(b)-5D), a mechanical behaviour that is consistent with microbial mats and not with a simple organic muck (Schieber, 1986). The gray interbeds, in contrast, behave mechanically like a fluid with the consistency of well stirred yoghourt, much more in keeping with a simple surficial mud deposit (these features are illustrated in Chapter 5).

In: *Atlas of microbial mat features preserved within the clastic rock record*, Schieber, J., Bose, P.K., Eriksson, P.G., Banerjee, S., Sarkar, S., Altermann, W., and Catuneau, O., (Eds.), Elsevier, p. 158-170. (2007)

The striped shales of the Newland Formation were deposited in a subtidal setting, basinwards of carbonates characterized by cryptalgal laminites, mudcracks, and flat pebble conglomerates (Schieber, 1986, 1998b). The microbial mats that gave rise to the carbonaceous silty shale beds colonized the shallow seafloor during periods of low sediment input. Comparison with modern muddy tempestites suggests that graded silt-clay couplets of the gray shale interbeds beds are storm deposits that intermittently interrupted the growth of subtidal benthic microbial mats (Schieber, 1986).

Whereas striped shales as decribed above are a common shale facies in the Newland Formation of the eastern Belt basin, locally a pyrite-enriched variant is also found. Pyritic striped shales are texturally analogous to "standard" striped shales (Fig. 7(b)-5A). They consist of layers of strongly pyritic shale that alternate with gray shale beds. The latter are identical in composition and sedimentary features to the gray shale interbeds in standard striped shales described above. When examined in detail, the pyritic beds have internal pyritic laminae whose wavy-crinkly texture is very similar in appearance to the wavy-crinkly laminae of standard striped shales (compare Figs. 7(b)-4D and -5B), suggesting that they have a comparable microbial mat origin. The iron enrichment in the pyritic striped shale facies is thought to reflect alluvial iron input along the basin margins (Schieber, 1985). Terrestrial runoff supplied iron in colloidal form as iron hydroxides to basin marginal lagoons. Iron hydroxide flocculates were incorporated into microbial mats and subsequently transformed into pyrite upon mat burial (Schieber, 1989). Excess iron input by terrestrial runoff can be documented for most of the Newland Formation (Schieber, 1995), but only in protected nearshore lagoons did it give rise to distinctive pyritic striped shales. More detailed information concerning pyrite formation during microbial mat diagenesis is provided in the chapter on mat decay mineralization (Chapter 5(e)).

The striped shales of the Newland Formation are probably the first well studied example of microbial mats in ancient mudstones, and since their original study (Schieber, 1986) comparable examples have been identified in other Proterozoic shale successions (e.g., Fairchild and Herrington, 1989; Logan et al., 1999; Banerjee et al., 2006; Sur et al., 2006; Patranabis-Deb et al., this volume). In addition, the Native Bee Siltstone of the Mid-Proterozoic Mount Isa Supergroup of Queensland, Australia, appears texturally quite similar to the striped shales of the Newland Formation (personal observations) and may have a comparable origin. The host rocks of several large Australian stratiform base metal deposits of Proterozoic age, such as Mt. Isa (Bennet, 1965; Mathias and Clark, 1975), Lady Loretta (Loudon et al., 1975), Hilton (Mathias et al., 1973), and McArthur River (Cotton, 1965; Murray, 1975; Lambert, 1976; Williams, 1978 a, b) are extensive pyritic shale deposits that have the same striped character as those pictured from the Newland Formation, and show the same wavy crinkly pyritic laminae within the pyritic beds. Although their microbial mat origin still needs to be established in each individual case through detailed study, the coincidence between pyritic striped shales and major base metal deposits is tantalizing (Schieber, 1990). The figures for striped shales presented in this section mainly describe their overall appearance at the outcrop and hand specimen scale, whereas the features critical for microbial mat identification are covered in detail in Chapter 5(a).

Revett Formation: iron stains and domes in sandstones

In various outcrops, sandstones of the Revett Formation (Fig. 7(b)-2) show conspicuous iron stains that are caused by the weathering of ferroan carbonate cements (siderite, ankerite, ferroan

dolomite) and pyrite. These sandstones formed in a fluviodeltaic setting with local development of sandy tidal flats, channel-mouth bar deposits, and barrier bars (Boyce, 1973; Bowden, 1977; Mumma et al., 1982; White et al., 1984). Most of the microbial mat features illustrated here were initially reported by Garlick (1988) who realized that the ferroan minerals in Revett sandstones were probably the diagenetic imprint of former microbial mats.

These ferroan minerals formed early in diagenesis (Hayes and Einaudi, 1986) as a result of reducing pore waters. In most sediments, reducing pore waters are due to contained organic matter. Initial organic matter degradation by aerobic bacteria consumes the available oxygen, and then anaerobic bacteria continue the process and foster precipitation of minerals such as ferroan carbonates and pyrite (e.g. Brett and Allison, 1998).

At the time the Revett Formation was deposited, microbial mats were the most likely producers of organic matter in shallow water sedimentary environments. Thus, early diagenetic reducing pore waters could have been generated in two ways: (1) through decay processes within a layer of sand that contained organic (microbial mat) debris (Berner, 1984), or (2) through decay processes in the lower portions of a microbial mat (e.g. Bauld, 1981; Gerdes et al., 1985).

As outlined in Chapter 4(d), microbial mats produce stratiform chemical boundaries that may be recognized in the rock record. Formation of “anoxic” minerals in the reducing pore waters beneath mats may thus produce thin, well defined, and laterally extensive horizons of minerals such as ferroan carbonates or pyrite. Observing such minerals in shallow water sandstones can therefore be a “tip-off” for the former presence of microbial mats (Gerdes et al., 1985; Garlick, 1988; Schieber, 1999).

The outcrop photos in Figure 7(b)-6 illustrate several features that can be associated with this type of mat record. The thin stratiform iron stains in Figure 7(b)-6A may be horizons produced by comparatively thin mats that colonized a sandy surface in between sedimentation events. The thicker layers in Figure 7(b)-6B, in contrast, have a more spotted (speckled) appearance which may reflect the decay of discrete organic particles (mat fragments) that were buried in an accumulating sand layer and led to localized reducing conditions as they decayed. This interpretation is supported by experiments that show (Chapter 8(c)) that physical diminution of eroded microbial mats during transport produces abundant millimetre-sized particles that are buried in associated sands.

Figure 7(b)-6C is from an exposure originally described by Garlick (1988), and shows what appears to be a scour depression that is filled with sand that has curved areas of iron stain. These are interpreted as the remains of curved microbial sand chips. These were presumably produced when microbial mats on sandy substrate desiccated, cracked, and formed abundant concave fragments. These fragments were entrained by the waters of a subsequent flood and redeposited and buried in a scour depression before they had a chance to soften again. Experimental work on transport of eroded microbial mats (Chapter 8(c)) suggests that they probably were transported for only a short distance (1-2 km at most) and buried within an hour of being eroded. Burial in water-saturated sediments enabled microbial degradation of the organic matter in these sand chips, led to localized reducing pore waters, and to precipitation of ferroan minerals.

Limonite stains with a contorted appearance (Fig. 7(b)-6D) are suggestive of sandstone intervals that experienced soft sediment deformation. Microbially bound sandstone surfaces behave like cohesive sheets under these conditions, rather than a simple mixture of sand and organic debris.

In places, Revett sandstones also formed dome-shaped buildups (Fig. 7(b)-7A) that are reminiscent of domal stromatolites reported from carbonates (e.g. Water et al., 1992). More commonly, however, iron stained mat layers are largely planar (Fig. 7(b)-6A) with minor local thickening (Fig. 7(b)-7B) that may be considered as incipient stromatolites of the type shown in Figures 7(b)-7A and -7C.

Mt. Shields Formation: ripple patches, iron stains, and domes

Wallace (1998) described the Mt. Shields Formation as a delta complex that prograded north into a shallow marine environment. Coarse sandstones were interpreted as deposited in delta-channel, delta-plain, delta-front, and strand-plain environments, fine sandstones were modelled as shallow marine deposits, and argillaceous and silty deposits ascribed to extensive shallow marine mudflats. In contrast, Winston (1986) has proposed a lacustrine interpretation. Yet, as summarized in the introduction to this chapter, the cumulative evidence suggests that the Belt Supergroup was deposited in an epicontinental basin that was connected to the Proterozoic ocean.

Although the Mt. Shields Formation is well known for bedding plane exposures with superbly preserved wave ripples, many sandstone bedding planes are nonetheless comparatively smooth and featureless. In a number of places these bedding planes show ripple patches (Fig. 7(b)-8A and -8B) that compare well to those described from mat stabilized tidal sand flats of Mellum island in the North Sea (Reineck, 1979), and to those described from the Cretaceous Dakota Sandstone (see this chapter, section 7(k)). This suggests that the smooth sandstone surfaces were mat stabilized as well, and that the ripple patches mark places where storms partially eroded the mat and enabled ripple formation in the underlying sand stratum.

In various locations, nearshore and coastal plain sandstones of the Mt. Shields Formation also show stratiform iron stained intervals that look very similar to those observed in sandstones of the Revett Formation (Fig. 7(b)-8C). They are likewise interpreted as the diagenetic testament of microbial mats that intermittently colonized and stabilized sandy surfaces.

Whereas microbial laminated layers in mudstones are in many instances planar due to the considerable post-depositional compaction that these rocks typically undergo, reddish and greenish mudstone-dominated intervals in the Mt. Shields Formation locally show domal features of considerable relief (Figs. 7(b)-9 and -10). These domal features are associated with mudstones that in addition to clay- and silt-rich laminae contain dolomite-rich laminae (Fig. 7(b)-9D). The latter contain variable amounts of finely crystalline dolomite, quartz silt, micas and clays and occur in domal buildups as well as in adjacent evenly laminated mudstones (Fig. 7(b)-9A and -B). Where these laminae are dolomite-dominated they show fenestral fabric (Fig. 7(b)-9D) and are indistinguishable from dolomite laminae in carbonate stromatolite horizons of the Mt. Shields Formation (Schieber, 1998b). The combination of randomly distributed and oriented micas, fenestrae, wavy-undulose laminae, and association with domal buildups suggest

that these laminae mark microbial mat stabilized sediment surfaces (Schieber, 1998b). Early cementation of dolomite-enriched laminae may have helped to preserve relief in clay-rich facies (Fig. 7(b)-9A and -B). In silt-rich facies (Fig. 7(b)-10C and -E), a smaller degree of post-depositional compaction probably contributed to preservation of low amplitude domes (Fig. 7(b)-9C).

The unusual raised rims of mudcrack polygons in some mudcracked intervals of the Mt. Shields Formation (Fig. 7(b)-10B) may also be a reflection of surficial microbial mats. They are unusual because there is relief on the order of 1-2 cm's between cracks and adjacent areas, whereas "normal" mudcracked intervals show negligible relief in comparison (Fig. 7(b)-10B). The raised polygon rims closely resemble cross-sections of polygonal mats from modern environments (Till, 1978). Upturned and uparched laminae adjacent to cracks look similar to what has been described as growth ridges from modern polygonal mats (Black, 1933; Ginsburg, 1960; Horodyski et al., 1977; Gerdes et al., 1993; see also Chapter 4, Figs. 4(c)-5 and -6). Standing water in the cracks promoted preferential microbial growth adjacent to cracks, and continued growth accentuated the ridges and led to formation of concave-upwards saucers. This scenario is also supported by the observation of dolomitic laminae of presumed microbial mat origin (see above). These dolomitic laminae are discussed further in the section on metabolic effects on mat structure (Chapter 4(b)).

McNamara Formation: ripple patches and pustular surfaces

The overall depositional setting of the McNamara Formation was probably similar to that proposed for the Mt. Shields Formation above, with an abundance of sea-marginal sandflats and deltaic environments. Sandstone surfaces with ripple patches (Fig. 7(b)-11A) have been observed in several places. Analogous to interpretation of these features in the Mt. Shields Formation (see above) and the Dakota Sandstone (Chapter 7(k)), they are considered to have resulted from partial erosion of a microbially bound sand surface.

Figure 7(b)-11B shows a sandstone bed with a variably "bumpy" surface. The "bumpy" areas may represent interference ripples, but there are also comparatively smooth areas that carry mm-scale wrinkles and pustules. In thin section, the uppermost centimetre of the sandstone bed consists of wavy-crinkly clay and silt laminae (Fig. 7(b)-11C). They resemble laminae seen in cross-sections of microcolumnar buildups or microbial tufts from modern mats (Gerdes and Krumbein, 1987). The interlaminated clay and silt (Fig. 7(b)-11D) indicates that this surficial layer had formed under conditions of lower and fluctuating energy, after the surface of the sandstone bed surface had been partially rippled.

Figures and Captions: Chapter7(b)

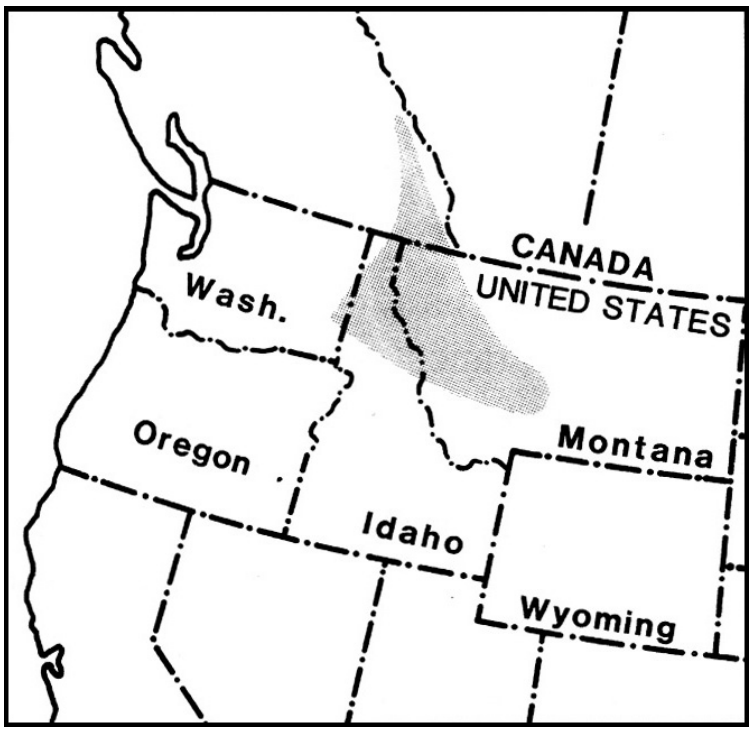

Figure 7(b)-1: Location of Belt Basin (stippled) and Belt Supergroup. Equivalent strata in Canada are known as the Purcell Supergroup.

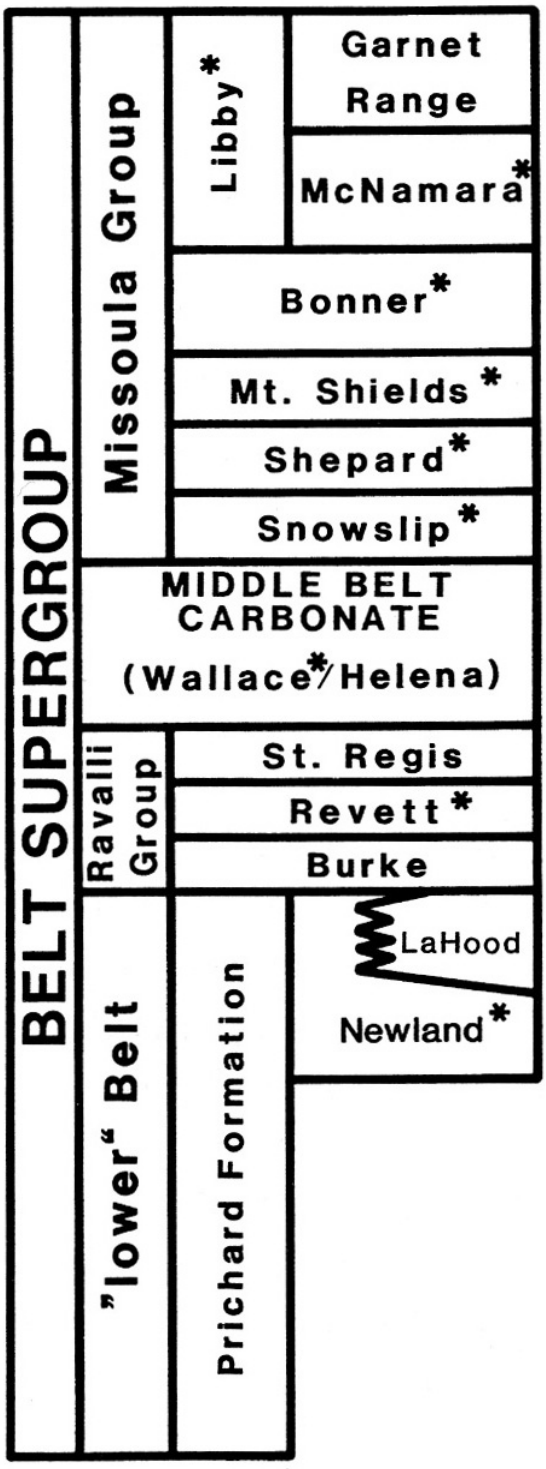

Figure 7(b)-2: Summary stratigraphic section of the Belt Supergroup. Star symbol indicates formations with microbial mat features in terrigenous clastics (Schieber, 1998b).

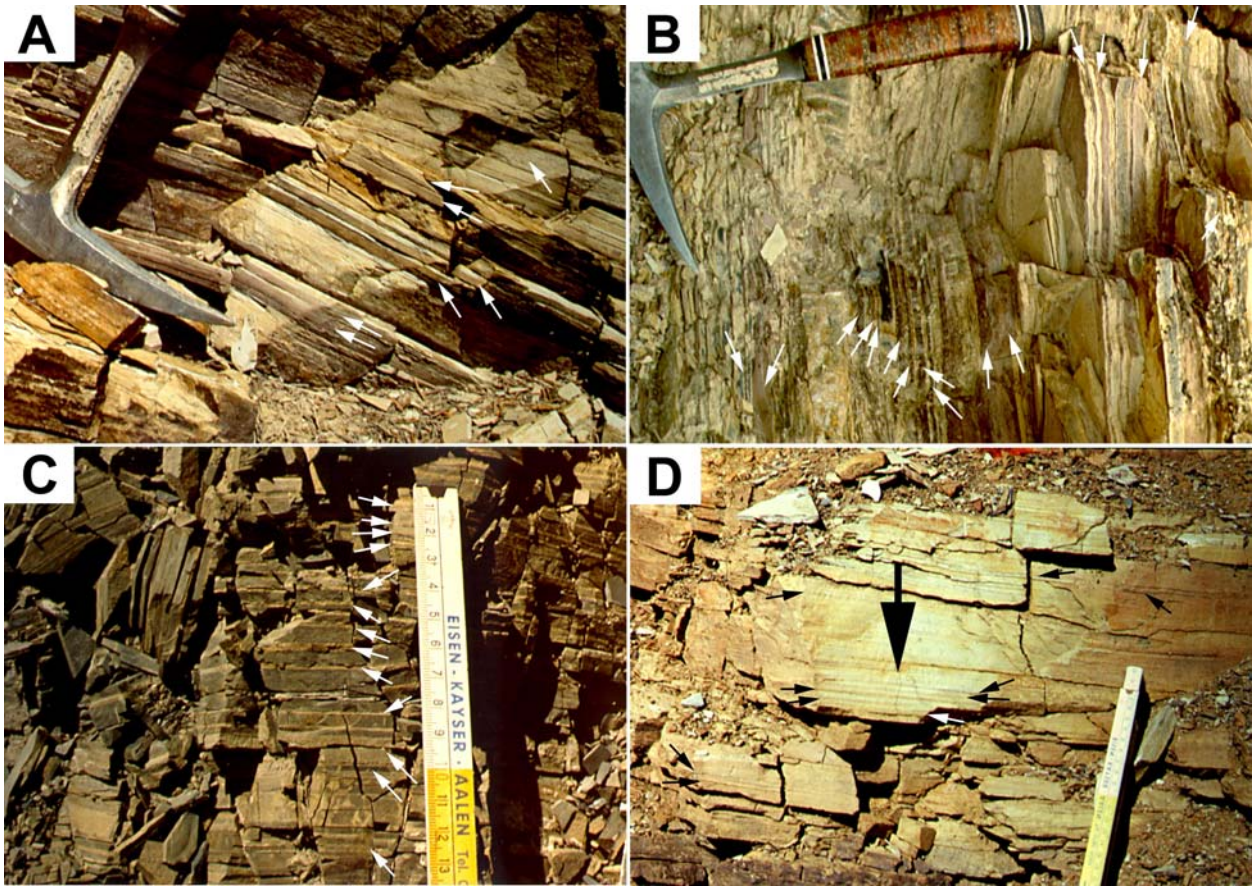

Fig. 7(b)-3: Newland Formation:

(A) Outcrop photo of striped shale from the Newland Formation, Big Belt Mountains, Montana. Shows reddish-brownish shale beds (marked with arrows) that alternate with gray shale beds. The reddish-brownish colours are due to oxidation of disseminated pyrite in these originally carbonaceous shale beds (see Fig. 7(b)-4). Hammer for scale.

(B) Outcrop photo of striped shale from the Newland Formation, Big Belt Mountains, Montana. Same locality as (A). Shows reddish-brownish shale beds (marked with arrows) that alternate with gray shale beds. The reddish-brownish colours are due to oxidation of disseminated pyrite in these originally carbonaceous shale beds (see Fig 7(b)-4). Hammer for scale. The weathered appearance of striped shales in (A) and (B) is very similar to the striped shales from the Tarur Nala Formation (Mid-Proterozoic of India, Fig. 7(d)-4).

(C) Outcrop photo of striped shale from the Newland Formation, Little Belt Mountains, Montana. The originally carbonaceous beds (marked with arrows) are light gray in this example, and interbedded with darker gray shales. The weathered carbonaceous-pyritic beds are also light gray in this example because iron was leached from these shales during weathering and thus did not produce the reddish stain observed in (A) and (B). Ruler has centimetre divisions.

(D) Outcrop photo of striped shale from the Newland Formation, Little Belt Mountains, Montana. Arrows point out weathered carbonaceous beds that alternate with gray shale beds. The

In: *Atlas of microbial mat features preserved within the clastic rock record*, Schieber, J., Bose, P.K., Eriksson, P.G., Banerjee, S., Sarkar, S., Altermann, W., and Catuneau, O., (Eds.), Elsevier, p. 158-170. (2007)

carbonaceous-pyritic beds become reddish stained during weathering, whereas the gray shales do not show much discolouration. The area below the large black arrow yielded specimens with pronounced wavy crinkly lamination, such as seen in Figure 7(b)-5. Ruler colour divisions (white-yellow) are 10 cm long.

In: *Atlas of microbial mat features preserved within the clastic rock record*, Schieber, J., Bose, P.K., Eriksson, P.G., Banerjee, S., Sarkar, S., Altermann, W., and Catuneau, O., (Eds.), Elsevier, p. 158-170. (2007)

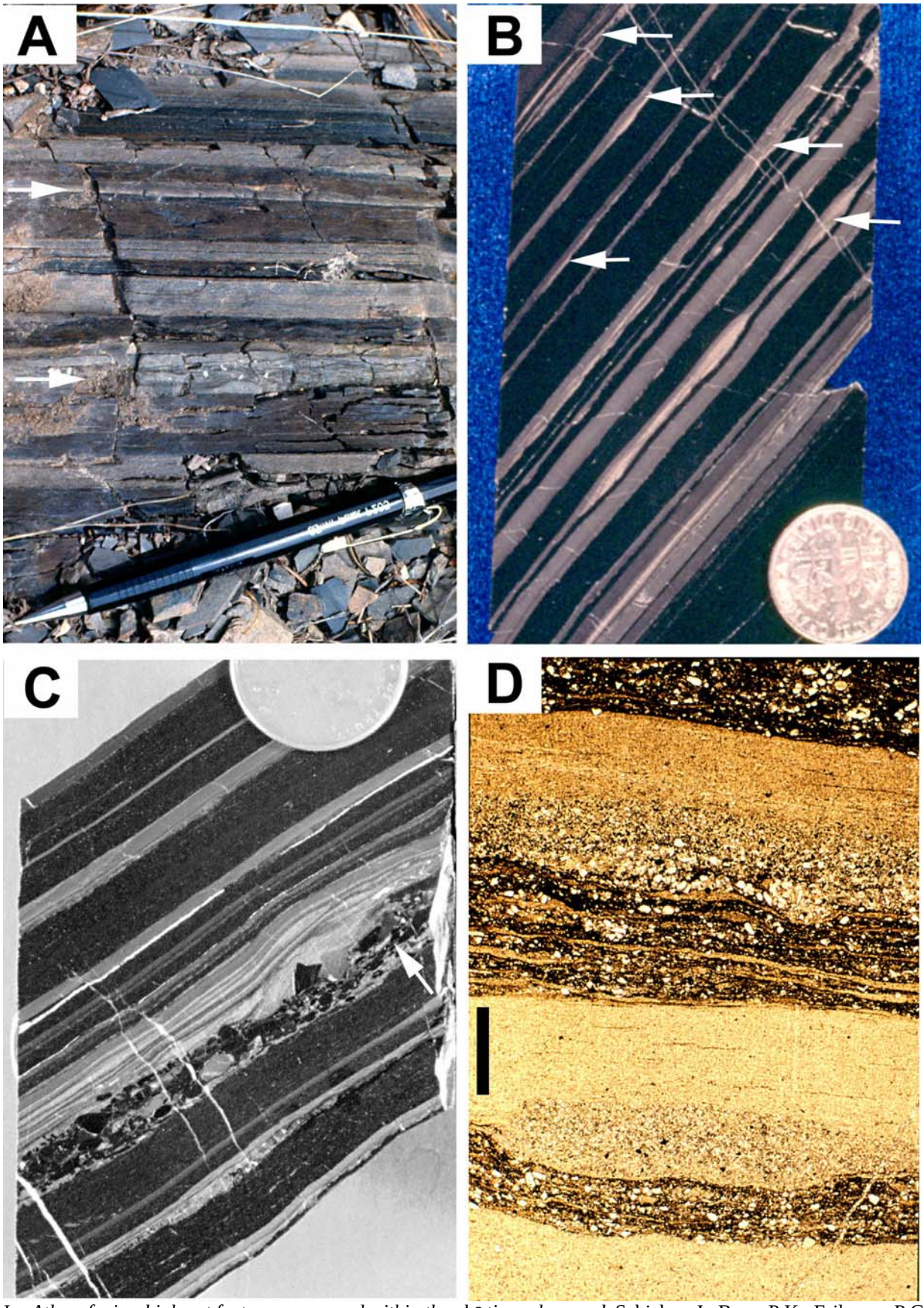

In: *Atlas of microbial mat features preserved within the clastic rock record*, Schieber, J., Bose, P.K., Eriksson, P.G., Banerjee, S., Sarkar, S., Altermann, W., and Catuneau, O., (Eds.), Elsevier, p. 158-170. (2007)

Fig. 7(b)-4: Newland Formation:

(A) Outcrop photo of striped shales in the Newland Formation of the eastern Belt Basin (Schieber, 1986). The dark layers are carbonaceous and internally laminated shales, whereas the gray layers consist of clay and silt and typically show normal grading. Arrows point to gray layers that exhibit normal grading with silt at the bottom of the layer. These shales are interpreted as reflecting growth of benthic microbial mats (dark layers) that was on occasion interrupted by high energy events (storms or floods) that deposited the gray layers. The pencil is 130 mm long.

(B) Photo of a cut and smoothed piece of drill core of striped shale. Shows the same layering as in (A). Graded silt/mud couplets are clearly visible (arrows), as well as ripples in the silty portion of gray layers. The coin is 18 mm in diameter.

(C) Photo of a cut and smoothed piece of drill core of striped shale. Arrow points to thick graded layer that contains shale clasts at its base, is overlain by laminated silt, and finally grades into gray clay. Probably a more proximal storm deposit. Coin is 18 mm in diameter.

(D) Photomicrograph of striped shale specimen. Shows very clearly the wavy-crinkly internal laminae of the dark carbonaceous layers (interpreted as benthic microbial mats). The non-carbonaceous inter-layers (clay/silt) show normal grading. Scale bar is 0.5 mm long. Because of the limited field of view of the typical petrographic microscope, a sample with very thin carbonaceous layers was chosen to illustrate the contrast between layer types.

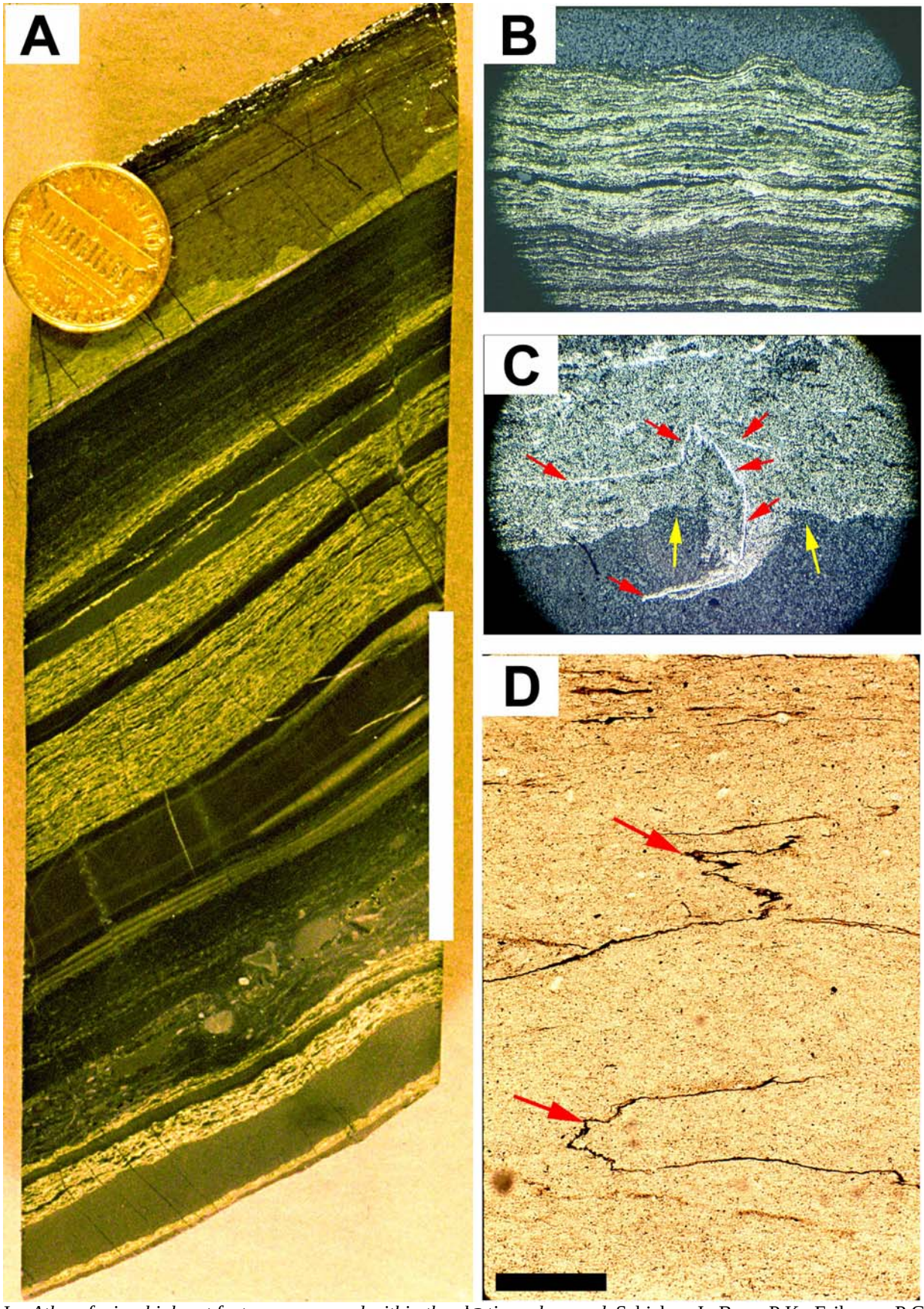

In: *Atlas of microbial mat features preserved within the clastic rock record*, Schieber, J., Bose, P.K., Eriksson, P.G., Banerjee, S., Sarkar, S., Altermann, W., and Catuneau, O., (Eds.), Elsevier, p. 158-170. (2007)

Fig. 7(b)-5: Newland Formation:

(A) Photo of drill core specimen of pyrite-mineralized striped shale (Schieber, 1989). Wavy-crinkly pyritic beds appear yellow and alternate with beds of dolomitic gray shale and a thick graded storm layer (white bar at right). The wavy-crinkly laminated pyritic beds are the direct facies equivalent of carbonaceous silty shale beds elsewhere in the striped shale facies, and are likewise interpreted as benthic microbial mat deposits. Coin is 19 mm in diameter.

(B) Photomicrograph of pyritic bed from (A). Shows wavy-crinkly lamination that texturally matches laminae observed in carbonaceous layers (interpreted as benthic microbial mats) from non-mineralized striped shales. Note load casts of overlying silt into underlying pyritic bed. Field of view is 7 mm in diameter.

(C) Pyritic bed of the type seen in (A) and (B) that has undergone soft sediment deformation. Soft sediment deformation has disrupted and homogenized the original laminated fabric, but already-cemented and "hardened" laminae (red arrows) were broken into plate-like bodies during soft sediment deformation, telescoped, and pushed into underlying and still soft shale bed. Upwelling of shale at locations marked with yellow arrows indicates that both the pyritic bed and the underlying shale were still unconsolidated when break-up of already hardened pyrite laminae occurred. These observations attest to a syndepositional origin of the laminated pyrite beds, not simply a diagenetic overprint of previously deposited carbonaceous shale beds. Field of view is 7 mm in diameter.

(D) Folded carbonaceous flakes (red arrows) in clayey shale. This suggests transport of thin, yet flexible pieces of carbonaceous material that measured as much as several centimetres across. In the Proterozoic, erosion of microbial mat surfaces would have produced fragments with those characteristics. Scale bar is 0.5 mm long.

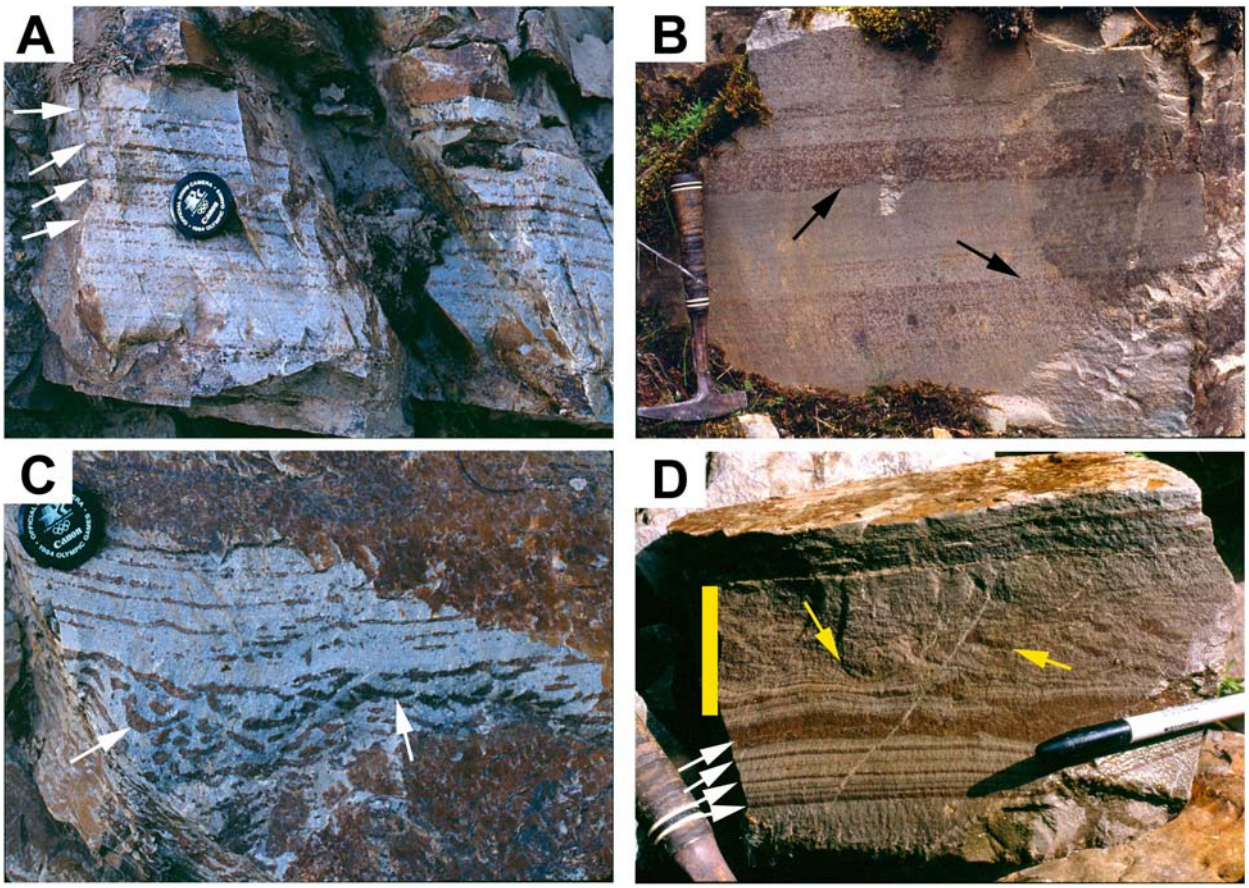

Fig. 7(b)-6: Revett Formation:

(A) Photo of medium-grained quartz arenite in Revett Formation. Arrows point to thin, bedding-parallel, iron stained (limonite) horizons that result from oxidation of ferroan carbonates (e.g. ankerite, siderite) and pyrite that are concentrated in pore spaces at these horizons. The very selective occurrence of these minerals at certain horizons is suggestive of mat decay mineralization (Schieber, 1999), formed beneath a surface sealing mat cover. Anoxic conditions are due to decay of organic matter beneath the active surface mat. Lens cap is 45 mm in diameter.

(B) Photo of medium- to fine-grained quartz arenite in Revett Formation. Two thicker horizons with abundant iron staining (limonite) pointed out by arrows. The sharp contrast between these horizons and the intervening sandstone interval suggests that there was originally abundant organic matter in the marked, iron-stained horizons. As in (A), the staining is due to oxidation of ferroan carbonates and pyrite. The more spotty nature of the iron stain suggests that the organic matter was in discrete particles that were mixed in with the sand during transport. The organic particles may have been derived from eroded and reworked mats. Hammer is 32 cm long.

(C) Scour depression in Revett Formation medium-grained quartz arenite. The depression is filled with curved elements (arrows) that have limonitic stain, overlain by sandstone with horizontal to wavy-undulose limonite stained layers, like those shown in (A). The latter are

interpreted as diagenetic (mat decay mineralization) remnants of thin microbial mats. The curved elements show sandstone with limonite and residual ferroan carbonate and pyrite cement, just like the limonite stained layers in (A) and (B). They are interpreted as remnants of desiccated and transported fragments of microbial mat that decayed after burial and led to the observed mineralization with ferroan carbonates and pyrite. Lens cap is 45 mm in diameter.

(D) Fine-grained quartz arenite in the Revett Formation. Shows an interval with soft sediment deformation (marked by yellow bar) that is sandwiched by sandstone with horizontal limonitic laminae (white arrows). Note fragments of contorted limonitic laminae (yellow arrows). Hammer is 32 cm long.

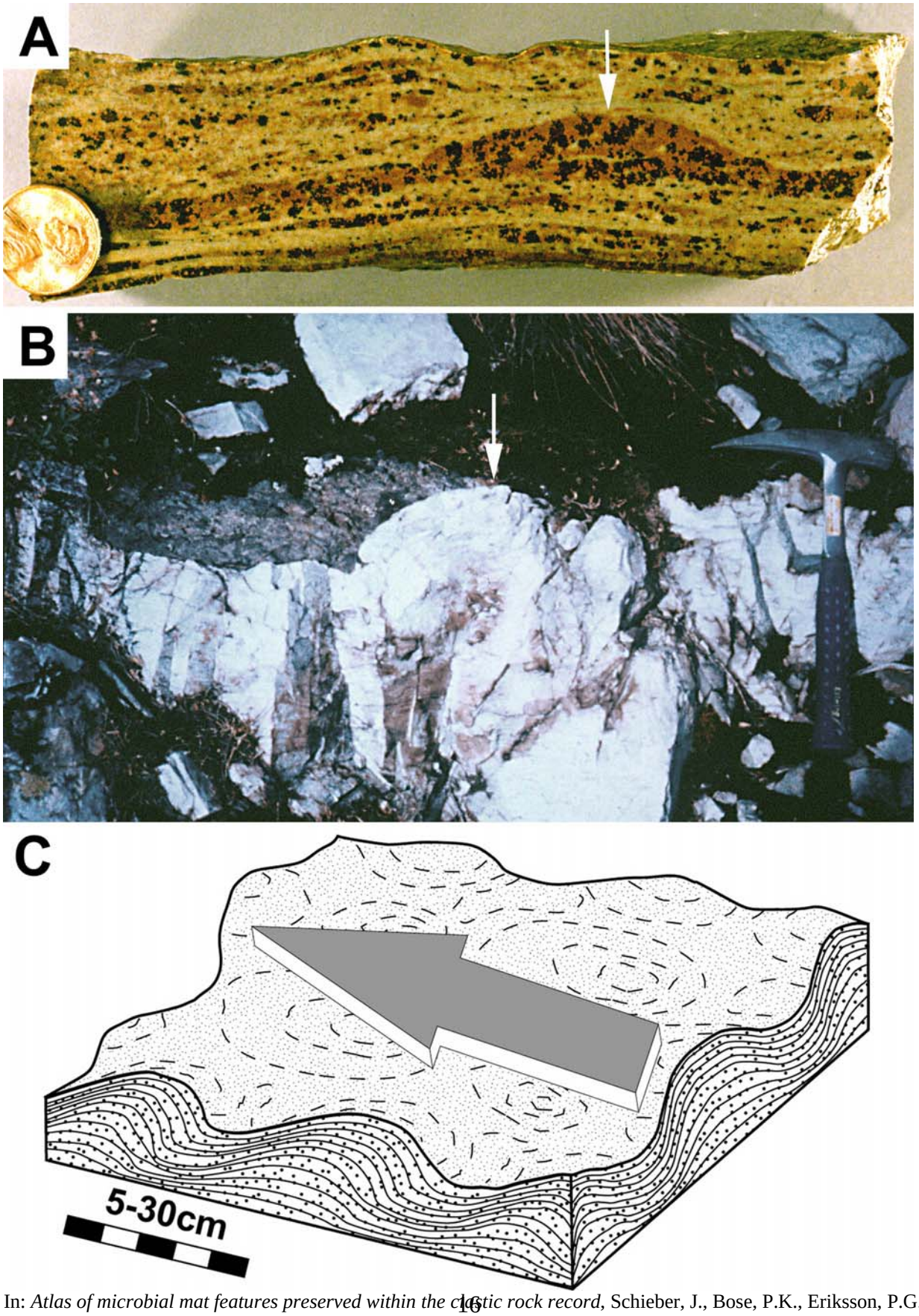

In: *Atlas of microbial mat features preserved within the clastic rock record*, Schieber, J., Bose, P.K., Eriksson, P.G., Banerjee, S., Sarkar, S., Altermann, W., and Catuneau, O., (Eds.), Elsevier, p. 158-170. (2007)

Fig. 7(b)-7: Revett Formation:

(A) Hand specimen of Revett Formation sandstone with iron stained (limonitic) laminae. The arrow points to a layer with asymmetric domal thickening, possibly an incipient stromatolite of the type shown in (A). The very dark patches are oxidized patches of siderite cement. The brownish-orange color of the laminae is due to more finely distributed iron oxides. The coin is 19 mm in diameter.

(B). Domal stromatolites in the upper portion of the Revett Formation near Troy, Montana. The hammer is 32 cm long. Photo courtesy of John Balla, ASARCO Inc.

(C) A sketch of a bed with domal features as seen in (B). Upward growth of mats is driven by competition for light, and as sediment is transported across the mat surface by currents it is trapped by the sticky mucilaginous mat surface. The latter results in preferred up-current growth of stromatolite laminae. From Schieber, 1999.

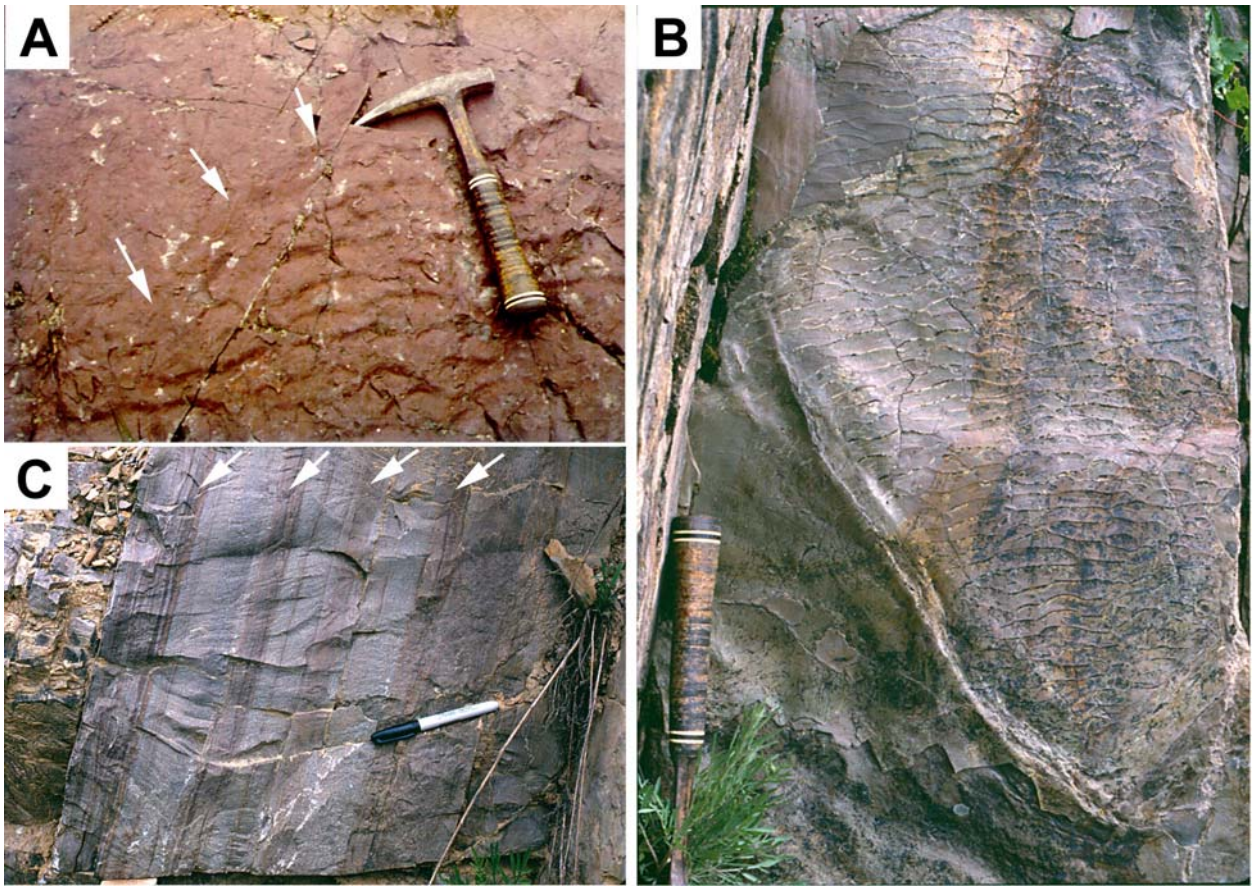

Fig. 7(b)-8: Mt. Shields Formation:

(A) Photo of the edge of a ripple patch in the Mt. Shields Formation. The photo shows the smooth transition between the rippled area and the non-rippled part of the bed surface. This type of margin is typical for other ancient and modern examples of ripple patches in microbially stabilized sand surfaces (e.g. Schieber, 1999). It indicates a contemporaneous origin of the two surface types and provides an argument for microbial mat stabilization of the non-rippled part of the bedding plane (Wunderlich, 1979). See also section 7(k). Hammer is 32 cm long.

(B) Photo of a patch of small ripples in otherwise smooth bedding plane of the Mt. Shields Formation. The rippled surface passes without physical break into the surrounding smooth area (lower right corner of image). The small wave length of the ripples suggests that these may be what Singh and Wunderlich (1978) described as mini-ripples, produced by slow moving waves in water only a few centimetres deep. Hammer handle is 180 mm long.

(C) Photo of a steeply dipping sandstone bed in the Mt. Shields Formation that has iron-stained intervals (marked with white arrows). The iron stain is due to oxidation of ferroan carbonate cement (ferroan dolomite, siderite) and/or dispersed diagenetic pyrite in these intervals. The strict stratiform distribution of these minerals indicates particularly reducing conditions in these horizons, possibly due to decay of organic matter beneath microbial mats that colonized these horizons. The marker pen is 135 mm long.

In: *Atlas of microbial mat features preserved within the clastic rock record*, Schieber, J., Bose, P.K., Eriksson, P.G., Banerjee, S., Sarkar, S., Altermann, W., and Catuneau, O., (Eds.), Elsevier, p. 158-170. (2007)

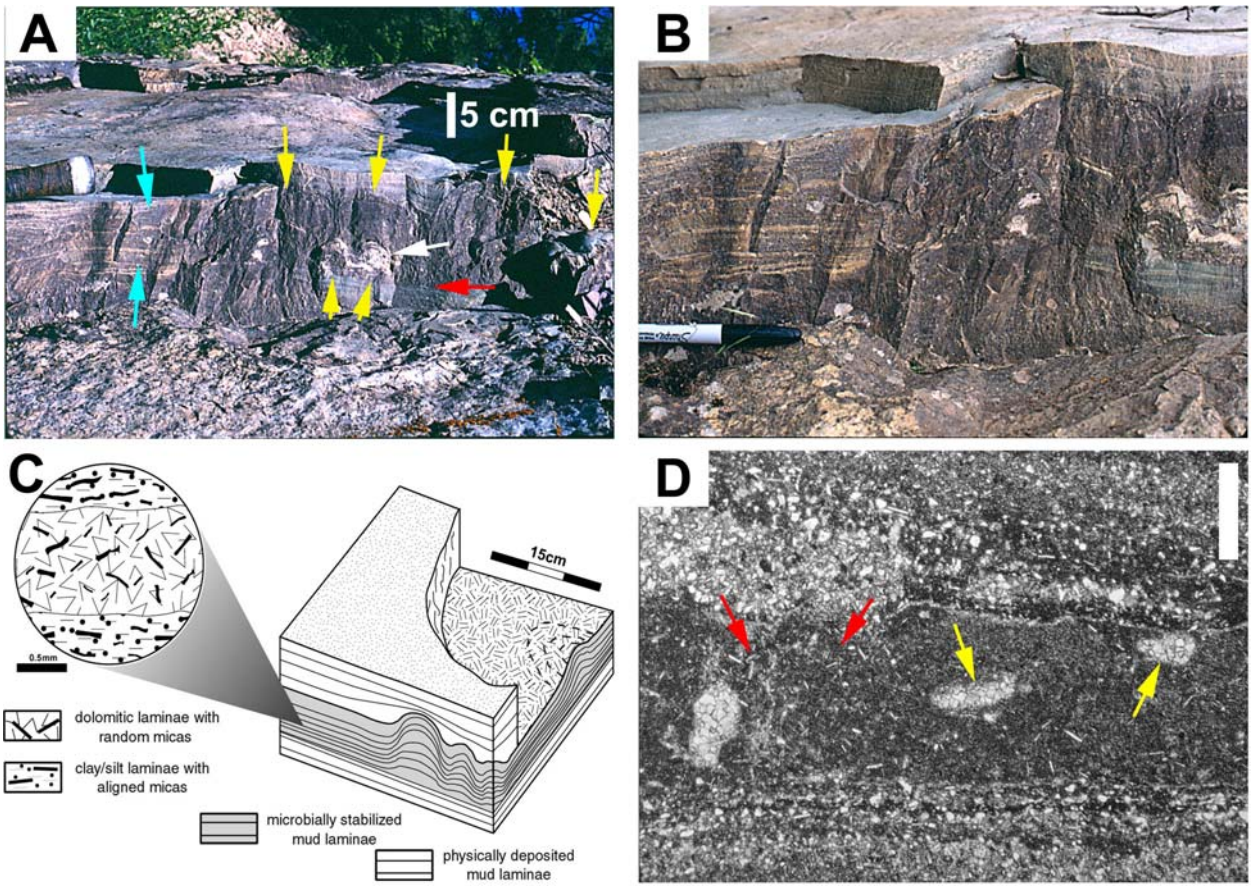

Fig. 7(b)-9: Mt. Shields Formation:

(A) Photo of greenish shale (argillite) of the Mt. Shields Formation with small stromatolite-like domal buildups (yellow arrows). These buildups developed on an originally flat surface (red arrow), show oversteepened laminae (white arrow), and laminae pass into surrounding horizontally laminated shale. The turquoise arrows bracket a package of horizontal laminae that is the lateral equivalent to the buildup laminae.

(B) Close-up photo of central portion of (A). Felt pen cap is 5 cm long (scale).

(C) Sketch of small domal buildups as seen in (A) and (B). It highlights oversteepened laminae at the edges of buildups. Those intervals that contain domal buildups are characterized by alternating dolomitic and clay/silt laminae (see detail drawing). The dolomitic laminae are interpreted (Schieber, 1998b) as fossil microbial laminae on the basis of randomly oriented mica flakes and fenestral fabric (see (D)). The shale (argillite) draping over these small domes consists only of clay and silt laminae; dolomitic laminae are absent. From Schieber, 1999.

(D) Photomicrograph of dolomitic lamina. Shows fenestrae filled with clear dolomite spar (yellow arrows). Red arrows point out area with abundant randomly oriented mica flakes. Scale bar 0.5 mm long. These laminae are thought to record microbial colonization of the mud surface (Schieber, 1998b).

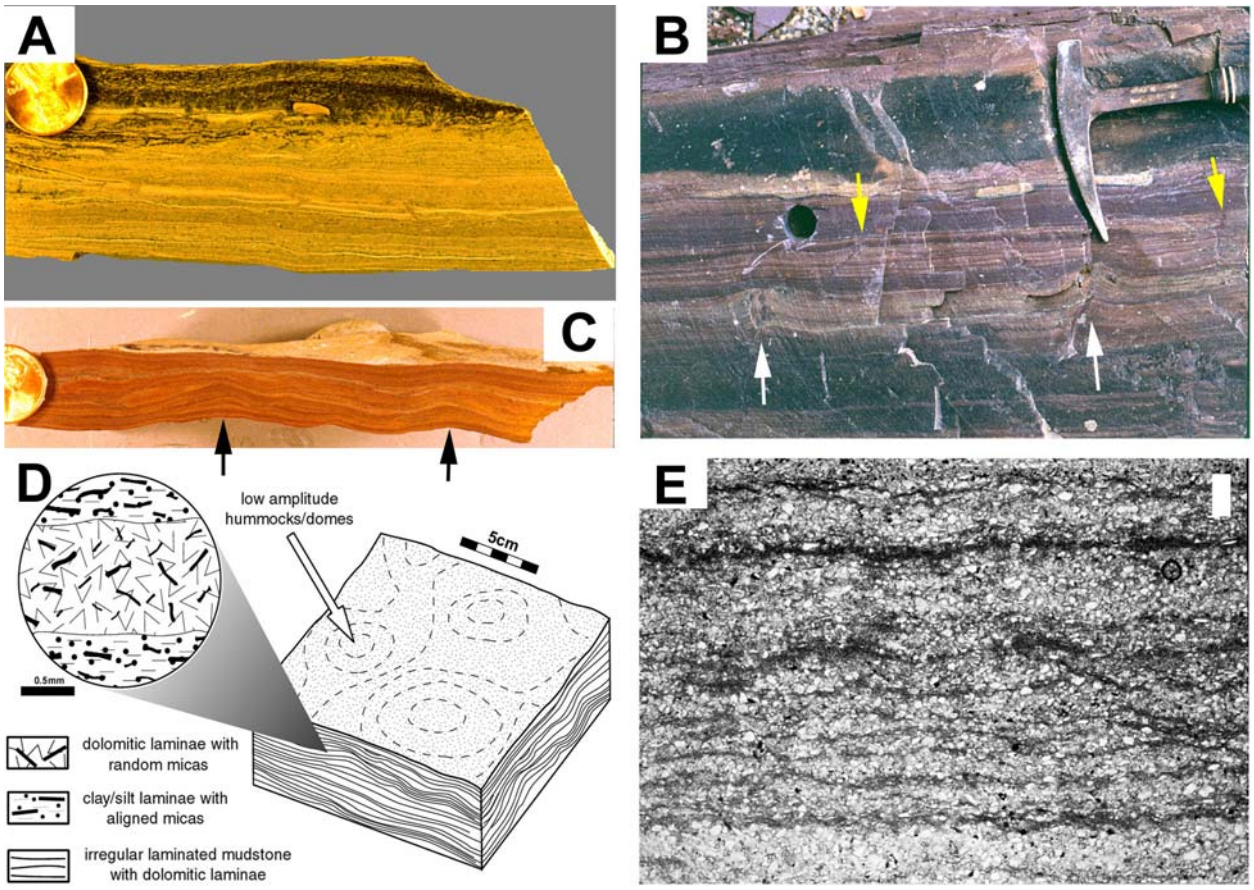

Fig. 7(b)-10: Mt. Shields Formation:

(A) Photo of sawed and smoothed sample of greenish Mt. Shields shale (argillite) with lighter coloured dolomitic laminae. The latter show randomly oriented mica flakes and in places fenestral fabric, and are interpreted as laminae that record microbial colonization of mud surfaces (Schieber, 1998b; see also Fig. 7(b)-9). Note that in the upper third of the sample weathering-related oxidation is obscuring the depositional fabric. Coin is 19 mm in diameter.

(B) Outrop photo of Mt. Shields Formation that shows interbedded sandstone beds (dark, massive appearance) and intervals of red shale (argillite). For one shale horizon, this photo shows uparched shale (argillite) laminae adjacent to mudcracks (white arrows). These are interpreted as microbially induced growth ridges (Gerdes et al., 1993). The area between the arrows resembles the cross-section of a polygonal stromatolite. Note for contrast the much smaller relief next to mudcracks in the overlying shale interval (yellow arrows). The lighter coloured laminae are dolomitic, show randomly oriented mica flakes, and are interpreted as microbial. Hammer head is 18 cm long.

(C) Photo of cut and ground specimen of red Mt. Shields shale (argillite). Note irregular lamina structure and small domal buildups (black arrows). Coin is 19 mm in diameter.

In: *Atlas of microbial mat features preserved within the clastic rock record*, Schieber, J., Bose, P.K., Eriksson, P.G., Banerjee, S., Sarkar, S., Altermann, W., and Catuneau, O., (Eds.), Elsevier, p. 158-170. (2007)

(D) Sketch that shows the low amplitude dome/hummocks seen in (C) in a three-dimensional context. The irregular laminae of these reddish shales (argillites) are characterized by alternating dolomitic and clay/silt laminae (see detailed drawing). Micas are aligned in terrigenous laminae, and random in dolomite laminae. The latter are interpreted as microbial in origin (Schieber, 1998b). From Schieber, 1999.

(E) Photomicrograph of fine sandy to silty laminae in Mt. Shields shale (argillite). Note wavy-crinkly laminae that contrast with the more planar laminae typical for physically deposited laminae. This style of lamination may indicate surface binding by microbial mats. Scale bar is 0.2 mm long.

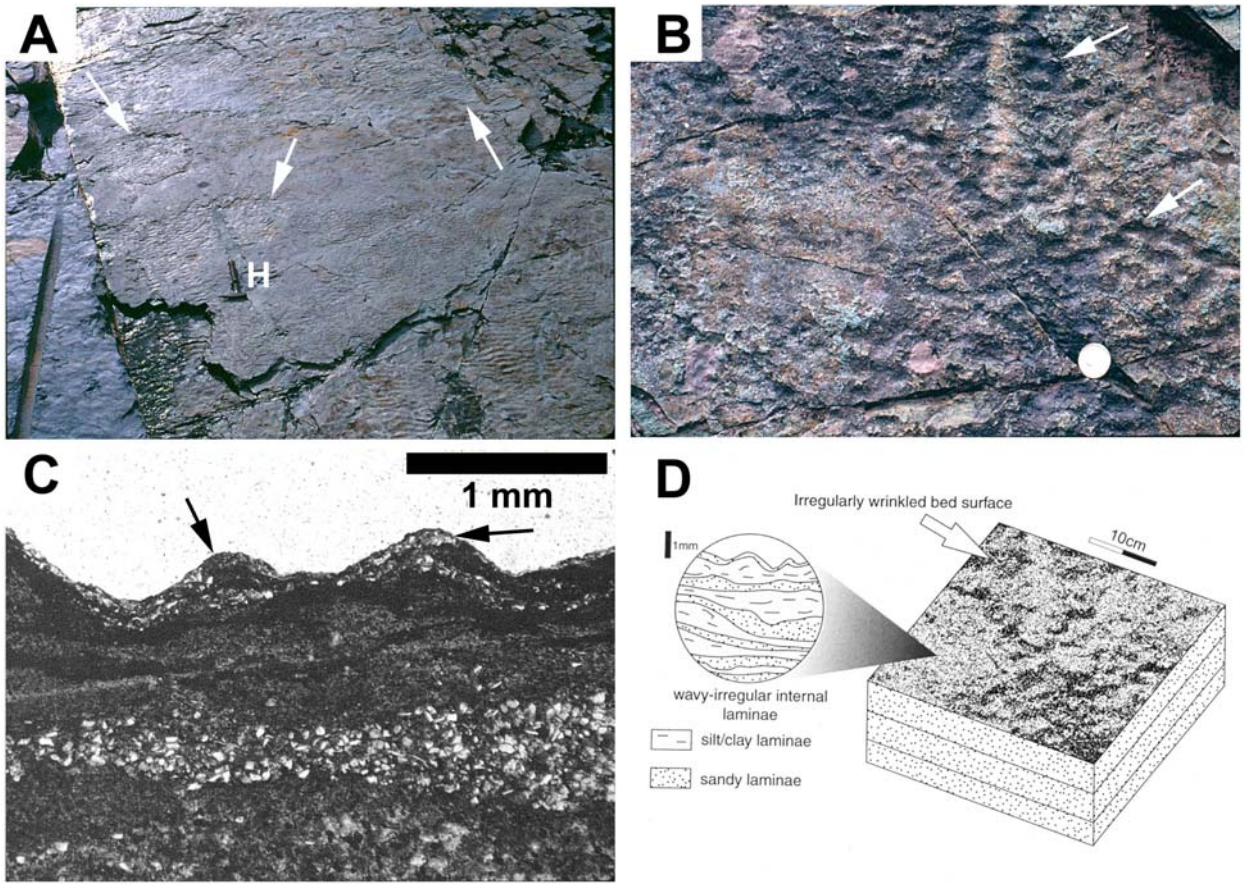

Fig. 7(b)-11: McNamara Formation:

(A) Ripple patches (arrows) on sandstone bedding plane in McNamara Formation. This bedding plane shows considerable resemblance to partially eroded microbially stabilized surfaces as illustrated by Reineck (1979) and Gerdes et al. (1985). The rippled surface above the hammer (marked H) passes without a break into the surrounding smooth surface (see D), an indication that the rippled surface and the smooth surface are contemporaneous. Hammer is 31.5 cm long.

(B) Pustular-crinkled bedding plane surface in fine sandstone of the McNamara Formation. Surface features pointed out by arrows probably represent rippled (interference ripples?) surfaces. In detail there is a pustular-crinkled surface morphology superimposed on these ripples (see (C) and (D)). Coin is 24 mm in diameter.

(C) Photomicrograph of thin section cut perpendicular to surface in (B). Note the mm-scale surface wrinkles (arrows) that contrast with laminae below surface. This surface morphology is superimposed on the larger scale ripple morphology, and is potentially of microbial origin.

(D) A sketch that contrasts the irregularly wrinkled/rippled bed surface seen in (B) (due to interference ripples) with the finely wrinkled surface morphology of presumed microbial origin as seen in (C). From Schieber, 1999.

References

Banerjee, S., Dutta, S., Paikaray, S. and Mann, U., 2006. Stratigraphy, sedimentology and bulk organic geochemistry of black shales from the Proterozoic Vindhyan Supergroup (central India). Journal of Earth Systems Science 115, p.37-48.

Bauld, J., 1981, Geobiological role of cyanobacterial mats in sedimentary environments: production and preservation of organic matter; BMR J. Austr. Geol. Geophys, v. 6, p. 307-317.

Bennet, E.M., 1965, Lead-zinc-silver and copper deposits of Mount Isa. In: McAndrew, J., (Ed.) Geology of Australian Ore Deposits, Commonw. Min. Metall. Congr., 8th, Melb., Vol. 1, pp. 1233-1246.

Berner, R. A., 1984, Sedimentary pyrite formation: An update: Geochimica et Cosmochimica Acta, v. 48, p. 605-615.

Black, M., 1933, The algal sediments of Andros Island, Bahamas. R. Soc. London Philos. Trans. Ser. B 222, p. 165-192.

Bowden, T.D., 1977, Depositional processes and environments within the Revett Formation, Precambrian Belt Supergroup, northwestern Montana and northern Idaho: University of California, Riverside, M.S. thesis, 161 p.

Boyce, R.L., 1973, Depositional systems in the Ravalli Group: a conceptual model and possible modern analogue: In: Belt Symposium 1973, Volume I: Idaho Bureau of Mines and Geology Special Publication 2, p. 139-158.

Brett, C.E., and Allison, P.A., 1998, Paleontological approaches to the environmental interpretation of marine mudrocks. In: J. Schieber, W. Zimmerle, and P. Sethi (editors), Shales and Mudstones (vol. 1): Basin Studies, Sedimentology and Paleontology, Schweizerbart'sche Verlagsbuchhandlung, Stuttgart, p. 301-349.

Cotton, R.E., 1965, H.Y.C. lead-zinc-silver deposit, McArthur Rover. In: McAndrew, J., (Ed.) Geology of Australian Ore Deposits, Commonw. Min. Metall. Congr., 8th, Melb., Vol. 1, pp. 197-200.

Cressman, E.R., 1989, Reconnaissance stratigraphy of the Prichard Formation (Middle Proterozoic) and the early development of the Belt Basin, Washington, Idaho, and Montana: U. S. Geological Survey Professional Paper 1490, 80 p.

Fairchild, I.J., and Herrington, P.M., 1989, A tempestite-stromatolite-evaporite association (Late Vendian, East Greenland) – a shoreface-lagoon model. Precambrian Research, v. 43, p. 101-127.

Garlick, W.G., 1988, Algal mats, load structures, and synsedimentary sulfides in Revett Quartzites of Montana and Idaho: Economic Geology, v. 32, p. 1259-1278.

Gerdes, G., and Krumbein, W.E., 1987, Biolaminated Deposits. Lecture Notes in Earth Sciences 9, Springer, New York, 183 pp.

Gerdes, G., Krumbein, W.E., and Reineck, H.-E., 1985, The depositional record of sandy, versicolored tidal flats (Mellum Island, southern North Sea). J. Sediment. Petrol., v. 55, p. 265-278.

Gerdes, G., Claes, M., Dunajtschik-Piewak, K., Riege, H., Krumbein, W.E., and Reineck, H.-E., 1993, Contribution of microbial mats to sedimentary surface structures. Facies, v. 29, p. 61-74.

Ginsburg, R.N., 1960, Ancient analogs of recent stromatolites. 21st Int. Geol. Congr. Copenhagen 22, pp. 26-35.

In: *Atlas of microbial mat features preserved within the clastic rock record*, Schieber, J., Bose, P.K., Eriksson, P.G., Banerjee, S., Sarkar, S., Altermann, W., and Catuneau, O., (Eds.), Elsevier, p. 158-170. (2007)

Harrison, J.E., 1972, Precambrian Belt Basin of Northwestern United States: its geometry, Sedimentation and Copper Occurrences: Geological Society of America Bulletin 83, p.1215-1240

Hayes, T.S., and Einaudi, M.T., 1986, Genesis of the Spar Lakestrata-bound copper-silver deposit, Montana; Part 1, Controls inherited from sedimentation and preore diagenesis: Economic Geology 81, p.1899-1931.

Horodyski, R.J., Bloeser, B., Von der Haar, S., 1977, Laminated algal mats from a coastal lagoon, Laguna Mormona, Baja California, Mexico. J. Sediment. Petrol, v. 47, p. 680-696.

Lambert, I.B. (1976). The McArthur zinc-lead-silver deposit: Features, metallogenesis and comparisons with some other stratiform ores. In: Wolf, K.H. (Ed.): Handbook of Strata-Bound and Stratiform Ore Deposits, Vol. 6, Elsevier, 535-585.

Logan, G.A., Calver, C.R., Gorjan, P., Summons, R.E., Hayes, J.M., and Walter, M.R., 1999, Terminal Proterozoic mid-shelf benthic microbial mats in the Centralian Superbasin and their environmental significance. Geoch. Cosmoch. Acta, v. 63, p. 1345-1358.

Loudon, A.G., Lee, M.K., Dowling, J.F., and Bourn, R., 1975, Lady Loretta silver-lead-zinc deposit. In: Knight, C.L. (Ed.), Economic Geology of Australia and Papua New Guinea, I Metals, Australas. Ins. Min. Metall. Mon. 5, pp. 66-74.

Mathias, B.V., and Clark, G.J., 1975, Mount Isa copper and silver-lead-zinc orebodies – Isa and Hilton Mines. In: Knight, C.L. (Ed.), Economic Geology of Australia and Papua New Guinea, I Metals, Australas. Ins. Min. Metall. Mon. 5, pp. 351-372.

Mathias, B.V., Clark, G.J., Morris, D., and Russel, R.E., 1973, The Hilton deposit – stratiform silver-lead-zinc mineralization of the Mt. Isa type. Bureau of Mineral Resources, Geology, and Geophysics, Bulletin 141, p. 33-58.

Mumma, M., Harbour, G. and Jayne, D., 1982, Prichard-Ravalli (Belt-Precambrian) sediments through space and time: In: R.R. Reid and G.A. Williams, editors, Society of Economic Geologists' Coeur d'Alene Field conference--1977: Idaho Bureau of Mines and Geology Bulletin 24, p. 1.

Murray, W.CJ., 1975, McArthur River H.Y.C. lead-zinc and related deposits. In: Knight, C.L. (Ed.), Economic Geology of Australia and Papua New Guinea, I Metals, Australas. Ins. Min. Metall. Mon. 5, pp. 329-339.

Schieber, J. 1985, The Relationship between Basin Evolution and Genesis of stratiform Sulfide Horizons in Mid-Proterozoic Sediments of Central Montana (Belt Supergroup). Dissertation, University of Oregon, Eugene, 811 pp.

Schieber, J., 1986, The possible role of benthic microbial mats during the formation of carbonaceous shales in shallow Proterozoic basins: Sedimentology, v. 33, p. 521-536.

Schieber, J., 1989, Pyrite mineralization in microbial mats from the Mid-Proterozoic Newland Formation, Belt Supergroup, Montana, U.S.A.: Sedimentary Geology, v. 64, p. 79-90.

Schieber, J., 1990, Pyritic shales and microbial mats: Significant factors in the genesis of stratiform Pb-Zn deposits of the Proterozoic? Mineralium Deposita, v. 25, p. 7-14.

Schieber, J., 1995. Anomalous iron distribution in shales as a manifestation of non-clastic fluvial iron supply to sedimentary basins: Relevance for pyritic shales, base metal mineralization, and oolitic ironstone deposits. Mineralium Deposita, v. 30, p. 294-302.

Schieber, J., 1998a. Sedimentologic, geochemical, and mineralogical features of the Belt Supergroup and their bearing on the lacustrine vs marine debate. In Belt Symposium III, R.B. Berg (ed.), Montana Bureau of Mines and Geology Special Publication 112, p. 177-189.

Schieber, J., 1998b, Possible indicators of microbial mat deposits in shales and sandstones: Examples from the Mid-Proterozoic Belt Supergroup, Montana, U.S.A. Sedimentary Geology, v. 120, p. 105-124.

Schieber, J., 1999, Microbial Mats in Terrigenous Clastics: The Challenge of Identification in the Rock Record. Palaios, v. 14, p. 3-12.

Singh, I.B., and Wunderlich, F., 1978, On the terms Wrinkle marks (Runzelmarken), Millimetre ripples, and mini-ripples. Senckenbergiana maritima, v. 10, p. 75-83.

Sur, S., Schieber, J., and Banerjee, S., 2006, Petrographic observations suggestive of microbial mats from Rampur Shale and Bijaigarh Shale, Vindhyan basin, India. Journal of Earth Systems Science, v. 115, p. 61-66.

Till, R., 1978, Arid shorelines and evaporites. In: Reading, H.G. (Ed.), Sedimentary Environments and Facies. Blackwell, Oxford, pp. 178-206.

White, B.G., Jeff Mauk, and Don Winston, 1984, Stratigraphy of the Revett Formation. In: S.W. Hobbs, editor, The Belt: Abstracts with Summaries, Belt Symposium II, 1983: Montana Bureau of Mines and Geology Special Publication 90, p. 16-17.

Williams, N., 1978a, Studies of the base metal sulfide deposits at McArthur River, Northern Territory, Australia: I. The Cooley and Ridge Deposits. Econ. Geol., v. 73, p. 1005-1035.

Williams, N., 1978b, Studies of the base metal sulfide deposits at McArthur River, Northern Territory, Australia: II. The sulfide-S and organic-C relationships of the concordant deposits and their significance. Econ. Geol., v. 73, p. 1036-1056.

Winston, D. 1986. Middle Proterozoic tectonics of the Belt basin, western Montana and northern Idaho. In Roberts, S. M. (ed.) Belt Supergroup: A Guide to Proterozoic Rocks of Western Montana and Adjacent Areas. Montana Bureau of Mines and Geology Special Publication 94, p. 245-257.

Wallace, C., 1998, Paleotransport directions and basin configuration, middle part of the Missoula Group (Belt Supergroup, Middle Proterozoic) western Montana. In Belt Symposium III, R.B. Berg (ed.), Montana Bureau of Mines and Geology Special Publication 112, p. 88-103.